Pergamon

0094-5765(94)00273-8

Acta Astronautica Vol. 35, No. 2/3, pp. 205–214, 1995

0094-5765/95 $9.50 + 0.00

AEROBRAKING TETHERS FOR THE EXPLORATION OF THE SOLAR SYSTEM†

J. M. LONGUSKI, J. PUIG-SUARI and J. MECHALAS
School of Aeronautics and Astronautics, Purdue University, West Lafayette, IN 47907, U.S.A.

Abstract—In previous work the authors developed a model for the analysis of orbiting tethered spacecraft in an atmosphere. This model was used to demonstrate the feasibility of the aerobraking tether concept for a mission to Mars. The present work studies the possibility of using such vehicles in the exploration of the other atmosphere-bearing planets and satellites in the solar system. This includes Venus, Jupiter, Saturn, Uranus, Neptune and Titan. After establishing ground rules, a study is performed in which the propellant mass for a typical rocket propulsion system is compared to the tether mass required for the aerobraking system. In every case, the tether mass turns out to be less than the propellant mass. The results have significant implications for the design of a new class of exotic spacecraft for the exploration of the solar system.

1. INTRODUCTION

Some of the more innovative work in the field of astronautics in the past few years has involved two new concepts which remain for the most part at a very theoretical stage. First, aerocapture has emerged as an interesting alternative to chemical propulsion in the exploration of the solar system, and currently is included in many of the proposals for manned missions to Mars. Second, tethers in space have generated tremendous interest, especially after the development of new composite fibers which make the construction of very long tethers feasible. The possibility that a tether could be used for aerobraking was first mentioned in the literature by Carroll[1]. The first analysis of a tether in an atmosphere was presented by Lorenzini *et al.*[2] and was limited to circular orbit around Mars. Puig-Suari and Longuski[3–5] analyzed the tether aerobraking system shown in Fig. 1. The system consists of an orbiter and an aerobraking probe connected by a thin tether. In the proposed maneuver, the probe flies through the atmosphere slowing the system down (from hyperbolic speed) to capture velocity. During fly-through, the orbiter remains significantly higher than the probe, above the sensible atmosphere.

In [3–5] the tether is assumed to be a rigid rod moving in the plane of the orbit. The exact equations of motion for this model were developed in[3]. These equations include distributed aerodynamic and gravitational effects on the tether, and allow for an arbitrary initial orbit. Numerical analysis of these equations for aerobraking at Mars showed that the aerobraking tether concept was physically feasible. Later work[5] focused on the development of simplified models to facilitate the search for initial conditions required to obtain aerocapture. The analysis determined that many different types of maneuvers, ranging from a vertical dumbbell to a horizontal drag chute, could produce aerocapture.

This paper analyzes the feasibility of aerobraking tethers for the exploration of the solar system, and compares the results with chemical propulsion systems. Simplified models are developed to determine the fly-through maneuver which minimizes the tether mass. The tether system is also designed to minimize the normal forces present in the rigid rod model, which would help to reduce bending in the (more realistic and complex) flexible tether. When these constraints are applied to the design a *unique configuration* is obtained. The resulting tether systems compare very favorably with the traditional chemical rockets.

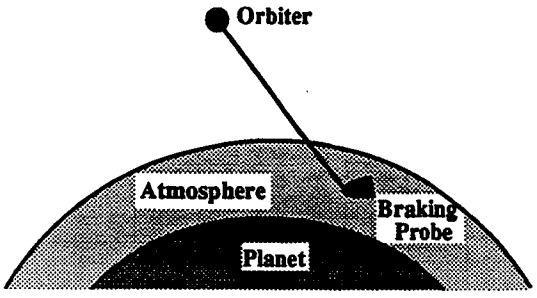

Fig. 1. Aerobraking tether.

†Paper IAF-92-1 presented at the *43rd Astronautical Congress*, Washington, D.C., U.S.A., 28 August–5 September 1992.

2. COMPARATIVE STUDY SPECIFICATIONS

The spacecraft chosen for the comparative study consists of an orbiter and a probe with a mass of 1000 kg each. This choice was arbitrarily made but reflects typical values for spacecraft used in the exploration of the solar system. It is assumed that the spacecraft reaches each planet via a Hohmann transfer, and at arrival a maneuver is performed to achieve capture into a near parabolic orbit ($e < 1$).

In the tethered system graphite is used because of its high strength and thermal resistance. Hercules AS4 graphite, which is currently available and has a tensile strength of 3.6 GN/m^2 and a density of 1800 kg/m^3, is chosen as representative of the type of material that could be used in the tether. This system will use the aerobraking tether maneuver to achieve capture. The orbiter is to be kept as high above the atmosphere as possible during the maneuver to avoid the need for aerodynamic shielding. The fact that the drag forces act mostly on the lower portion of the tether results in a large torque that tends to rotate the system and could easily plunge the orbiter into the atmosphere. Previous research [5] found that this could be prevented by giving the system an opposite spin rate before impact. After the impact the spin rate can be eliminated as was shown in [5], but since tension due to centripetal forces is produced by spin, some analysis is required to determine the best spin-in/spin-out combination (Fig. 2) to minimize tether mass. The model in [3] provides the forces acting on the tether at the two end points. These forces will be used to determine the strength requirements on the tether. Both tensile and normal forces are computed since the model assumes the tether to be a rigid rod. The presence of normal forces on the tether is not desirable because if a flexible tether was used it would bend to accommodate those forces. Therefore, the normal forces should be minimized in order to minimize the bending of a more realistic flexible tether. For the purpose of this analysis, the drag coefficients for the probe, tether and orbiter are assumed to be ([2,3]) $C_{Dp} = 1$ and $C_{Dt} = C_{Do} = 2$.

The tether system will be compared to a chemical rocket system which uses propellant to capture the orbiter around the planet. The probe, is assumed to use aerobraking to achieve capture in the same manner as the Galileo probe currently enroute to Jupiter. In order to reflect current technology a specific impulse of 300 s is chosen.

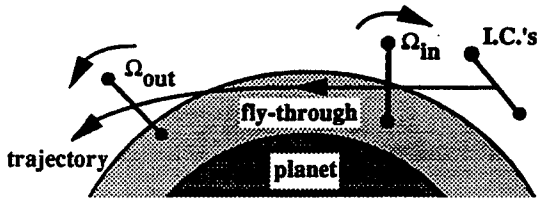

Fig. 2. Aerobraking maneuver.

The comparison will be based on the masses of the tether and the propellant. The relative masses of the equipment involved in each case, such as tanks and nozzles in the propulsive system, and reel and deployment equipment in the tethered system, are assumed to be similar and therefore will be ignored. Some questions may arise about the validity of this comparison. For example, the tether spin rate increases the velocity of the probe which raises its heat shielding requirements when compared with the probe in the propulsive case. On the other hand, the near parabolic capture orbit favors the propulsive system since to get into a more realistic orbit extra fuel would be required, where the tethered system could achieve (at no cost) a lower eccentricity orbit in a second aerobraking pass. The tether mass versus propellant mass study is chosen as a simple way to evaluate the performance of the tethered system. The favorable results presented in this analysis will be followed up with a more detailed examination.

3. TETHER DESIGN CONSIDERATIONS

3.1. Equations of motion

The equations of motion for a tethered system in an atmosphere are derived in [3]. The complete equations of motion for such a system are extremely complex, even with the following simplifying assumptions. First, since the spacecraft are small compared with the dimensions of the complete system, the orbiter and the probe are analyzed as particles. Next, the motion of the system is constrained to the plane of the orbit. Disturbances in the out-of-plane direction are small, which makes this a reasonable assumption. In addition, the orbit is assumed to be equatorial and the atmosphere is assumed to rotate with the planet. Also, the tether is modeled as a rigid rod. This assumption is often made in the literature and has been shown to be reasonable in most cases [2]. The analysis includes the aerodynamic effects of an atmosphere on the system, assuming an exponential atmospheric density model of the form:

$$\rho_i = \rho_r \, e^{(H_r - R_i + R_{pl})/H} \tag{1}$$

where ρ_i represents the density at a radius R_i from the center of a planet with radius R_{pl}, ρ_r is the reference density at a reference altitude H_r and H is the scale height. The drag forces acting on the system are assumed to be of the form:

$$\mathbf{F} = -\tfrac{1}{2}\rho C_D S V \mathbf{V} \tag{2}$$

where C_D is the drag coefficient, S represents the frontal area of the body and $\mathbf{V}$ is the velocity with respect to the atmosphere. When the drag effects on the tether are analyzed, the drag forces must be integrated over its length since the wind velocity and the atmospheric density change continuously along the tether. The exact form of this integral is derived in [3], and has no closed form solution. Approximate expressions for the integral are found to reduce the

resulting integro-differential equations to non-linear differential equations with time-varying coefficients. Integration of the drag forces is not required for the orbiter and the probe, since they are analyzed as particles. The gravitational forces on the system are obtained using an inverse square model. The gravity force analysis on the tether also requires integration over its length, but in this case a closed form expression can be obtained for the integral coefficients. The equations of motion for this system are developed using a newtonian approach and are too lengthy to be shown here (most of [3] is devoted to the derivation of these equations). The simulations of the tether maneuvers shown in this paper are obtained by numerically integrating the equations of motion presented in [3].

The analysis in [5] indicates that the aerodynamic effects acting on the tether resemble impulses, hence, for preliminary design purposes, the fly-through maneuver can be approximated as an impact problem. In the spinning tether case, the centripetal forces due to spin may (depending on the maneuver) produce most of the tension forces. This observation can also be used to simplify the design analysis. Finally, given an exponential atmosphere, most of the aerodynamic effects take place near the probe. All these facts can be used to derive very simple models which are applied to the aerobraking tether feasibility study in this paper. Thus certain "rules of thumb" emerge which guide the tether design for aerobraking at various planets.

3.2. *Spin rate analysis*

The question arises: what values of spin-in, Ω_{in}, and spin-out, Ω_{out}, minimize tether mass (see Fig. 2)? To answer this question, first, assume that all the tension on the tether is due to spin, that is, ignore gravitational effects. Then, approximate the maneuver as an impact acting on the probe while the tether is in a local vertical orientation as shown in Fig. 3. Finally, neglect the mass of the tether since it is small compared to that of the orbiter and the probe. The value of the impulse P can be computed using the fact that it must slow the system down to capture velocity and that the magnitude of the required ΔV is known. Hence, P can be written as:

$$P = (m_o + m_p)\Delta V \tag{3}$$

where m_o and m_p are the masses of the orbiter and the probe, respectively. The angular impulse A due to P is:

$$A = Pl_p = (m_o + m_p)\Delta V l_p = I\Delta\Omega \tag{4}$$

where $\Delta\Omega$ is the change in angular velocity (spin) and I is the moment of inertia of the system given as:

$$I = m_o l_o^2 + m_p l_p^2 \tag{5}$$

l_o and l_p are the distances from the orbiter and the probe to the center of mass of the system and are given by:

$$l_o = \frac{m_p}{m_o + m_p} l, \quad l_p = \frac{m_o}{m_o + m_p} l \tag{6}$$

where l is the total length of the tether. Note that these expressions do not include the mass of the tether which is ignored in this part of the analysis. After some algebra we obtain an expression for $\Delta\Omega$ as a function of ΔV:

$$\Delta\Omega = \frac{m_o + m_p}{m_p l}\Delta V \tag{7}$$

The tension on the tether produced by the spin rate is:

$$T = \frac{m_o m_p}{m_o + m_p} l\Omega^2 \tag{8}$$

Note that this is an expression for the tension at the ends of the tether, but, since the tether is assumed to be massless, the tension is constant along the tether. The maneuver should be designed to minimize the tension on the tether, that is, minimize the maximum value of the tensions due to Ω_{in} and Ω_{out}. The difference between Ω_{in} and Ω_{out} is given by eqn (7). Clearly minimum tension is achieved when

$$\Omega_{in} = -\Omega_{out} \tag{9}$$

In [5] a maneuver design with $\Omega_{in} = \Delta\Omega$, and $\Omega_{out} = 0$ was analyzed. This option has some advantages (i.e. no spin after the fly-through) but the maximum tension is increased by a factor of four [compared to condition (9)]. When the spin rates are matched, by using eqns (7) and (8), the tension on the tether can be expressed explicitly as a function of ΔV:

$$T = \frac{m_o(m_o + m_p)}{4m_p l}\Delta V^2 \tag{10}$$

The tether diameter is now determined as a function of the strength of the material chosen, since it should

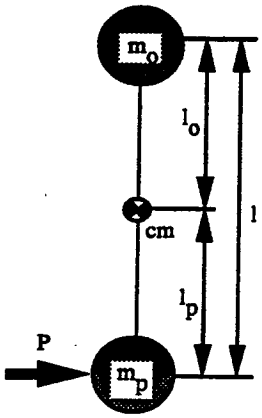

Fig. 3. Tether orientation during fly-through.

be designed to withstand the tension given in eqn (10). The expression relating tether diameter, d, to ΔV is:

$$d^2 = \frac{m_o(m_o + m_p)}{\pi m_p \sigma_u l} \Delta V^2 \tag{11}$$

where σ_u is the ultimate strength per unit area of the tether material. The total mass of the tether, m_t, is:

$$m_t = \frac{\rho_t m_o(m_o + m_p)}{4\sigma_u m_p} \Delta V^2 \tag{12}$$

where ρ_t is the density of the tether material. Note that the length of the tether is not contained in the tether mass expression. That is, the mass of the tether is determined only by the value of ΔV, the masses of the orbiter and the probe, and the properties of the tether material, σ_u and ρ_t. Thus, from eqn (12), we see that, for a given material, *the mass of the tether is not affected by its length*. The reason for this is that, for a given ΔV, as the tether length is increased the tension (due to centripetal acceleration) decreases proportionally with l^{-1}, whereas the mass increases with l, so the two effects cancel.

3.3. Normal force analysis

The tether model used for the simulations in this paper, which is derived in [3], assumes the tether to be a rigid rod. The model also provides the tether forces acting on the orbiter and the probe. These forces have components in both the longitudinal and the normal directions due to the rigid tether model. A more realistic model for the tether would include flexibility, allowing bending if normal forces were present. Bending is not desirable, since it would change the tether length (orbiter altitude), drag characteristics, and perhaps, some of the other basic modeling assumptions. In order to reduce this problem, the possibility of eliminating, or minimizing (by design), the normal forces is studied.

3.3.1. Center of percussion/center of pressure matching. First, the normal forces at the orbiter end are studied. Some simplifying assumptions are made to facilitate this analysis. The tethered system is assumed to remain in a vertical orientation during the fly-through maneuver, which is the optimum orientation to keep the orbiter away from the sensible atmosphere. Also, the orbiter radius and velocity are assumed to be constants throughout the maneuver, which are approximated by the orbital conditions around periapsis where the fly-through occurs. At this point, if the drag effects are considered approximately impulsive, it is clear that the normal forces disappear if they act at the center of percussion about the orbiter. Therefore, the normal forces at the orbiter end are minimized when the center of pressure (where the resultant of all the drag forces acts) and the center of percussion are located at the same point on the tether. The position of the center of percussion

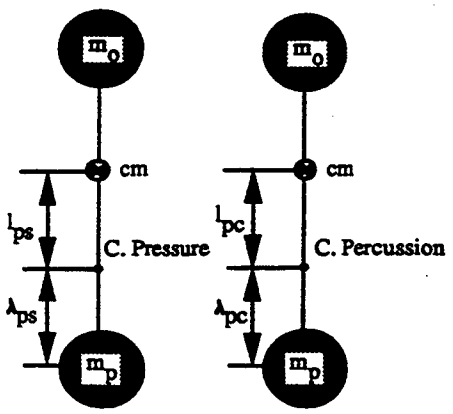

Fig. 4. Locations of center of pressure and center of percussion.

about the orbiter with respect to the center of mass of the system, l_{pc}, is (Fig. 4):

$$l_{pc} = I/(ml_o) \tag{13}$$

where I is the moment of inertia of the system about the center of mass and m is the total mass. If the tether is assumed massless, then the center of percussion of the system about the orbiter is located at the probe. When the mass of the tether, m_t, is included, the center of percussion moves towards the center of mass. The distance it moves from the probe, λ_{pc}, is given by:

$$\lambda_{pc} = l_p - l_{pc} = l_p - I/(ml_o) \tag{14}$$

where the I and m are:

$$I = m_p l_p^2 + m_o l_o^2 + (1/3)m_t(l_o^3 + l_p^3)/l$$
$$m = m_o + m_p + m_t \tag{15}$$

Note that when the mass of the tether is included in the analysis, the expressions for l_p and l_o become:

$$l_p = \frac{m_o + \frac{1}{2}m_t}{m} l, \quad l_o = \frac{m_p + \frac{1}{2}m_t}{m} l \tag{16}$$

The position of the center of pressure is found by combining the drag effects acting on the probe and the tether. The effects on the orbiter are negligible since it is located at a much higher altitude than the probe. The drag forces on the probe and the tether can be found using expressions derived in [3] and the approximations mentioned above:

$$F_{Dp} = -\tfrac{1}{2}\rho_r C_{Dp} S_p (R - l_p)^2 \dot{\theta}^2 \times e^{(H_r + R_{pl} - R + l_p)/H} \tag{17}$$

$$F_{Dt} = -\tfrac{1}{2}\rho_r C_{Dt} d\, e^{(H_r + R_{pl} - R)/H} \times H\dot{\theta}^2[R^2\gamma_1 + 2R\gamma_2 + \gamma_3] \tag{18}$$

with

$$\gamma_1 = -e^{-l_o/H} + e^{l_p/H}$$
$$\gamma_2 = -(l_o + H)\, e^{-l_o/H} - (l_p - H)\, e^{l_p/H}$$
$$\gamma_3 = -(l_o^2 + 2H(l_o + H))\, e^{-l_o/H} + (l_p^2 - 2H(l_p - H))\, e^{l_p/H} \tag{19}$$

where C_{Dp} and C_{Dt} are the drag coefficients of the probe and the tether respectively, S_p represents the frontal area of the probe, and R and $\dot{\theta}$ are the orbital radius and angular rate of the center of mass. The tether drag force is distributed along the length and the tether center of pressure must be found to obtain the center of pressure of the total system (tether plus probe). The position of the center of pressure of the tether (Fig. 4) with respect to the center of mass of the system, l_{tps}, is given by the ratio of the drag force (18) and drag moment on the tether derived in [3] which, with the assumptions made previously, is:

$$M_{Dt} = -\tfrac{1}{2}\rho_r C_{Dt} d\, e^{(H_r + R_{pl} - R)/H} \times H\dot{\theta}^2[R^2\gamma_2 + 2R\gamma_3 + \gamma_4] \quad (20)$$

where

$$\gamma_4 = -[l_o^3 + 3Hl_o^2 + 6H^2(l_o + H)]\, e^{-l_o/H} - [l_p^3 - 3Hl_p^2 + 6H^2(l_p - H)]\, e^{l_p/H}$$

Then the expression for l_{tps} becomes:

$$l_{tps} = \frac{R^2\gamma_2 + 2R\gamma_3 + \gamma_4}{R^2\gamma_1 + 2R\gamma_2 + \gamma_3} \quad (21)$$

The position of the tether center of pressure with respect to the probe, λ_{tps}, is given by:

$$\lambda_{tps} = l_p - l_{tps} \quad (22)$$

Note that, in the limit, as the tether length goes to infinity the value of λ_{tps} goes to H, the scale height of the atmosphere. That is:

$$\lim_{l \to \infty} \lambda_{tps} = H \quad (23)$$

Finally, the position of the center of pressure of the complete system with respect to the probe, λ_{ps}, is:

$$\lambda_{ps} = F_{Dt}\lambda_{tps}/(F_{Dp} + F_{Dt}) \quad (24)$$

In order to minimize the normal forces at the orbiter end of the tether, the values of λ_{pc} and λ_{ps} should be equal, that is the center of pressure and the center of percussion should match. We call this requirement *center matching*.

3.3.2. Aeromatching. At the probe end of the tether the normal force analysis is much simpler. Normal forces at the tether end are present when the tether and the probe have different aerodynamic force-to-mass ratios. This means that the decelerations that the atmosphere produces on them are different and, since they must move together, normal forces appear in the rigid rod model. The atmospheric density and wind velocity at the end of the tether are the same for both, the probe and the tether. Therefore, from the aerodynamic force expression, the condition that eliminates the normal forces can be found by equating the ballistic coefficients:

$$\beta/(C_{Dt}d) = m_p/(C_{Dp}S_p) \quad (25)$$

where β is the tether linear density, which depends on the tether mass and its dimensions. We call this condition *aeromatching*.

4. INTERPLANETARY MISSIONS

The missions to the various planets are determined by assuming a Hohmann transfer from a 200 km Earth parking orbit. The return mission from Mars to Earth consists of the second "leg" of the transfer ellipse from the Earth to Mars mission. The mission to Titan assumes tether braking at Titan in order to achieve capture at Saturn. All the planets are assumed to have co-planar, circular orbits about the Sun with the semi-major axes used as the orbital radii. The ΔV needed to go from the incoming hyperbolic trajectory to a parabolic trajectory is found by using a patched-conic solution, and is given by the expression

$$\Delta V = \sqrt{\frac{2\mu}{r_p} + V_\infty^2} - \sqrt{\frac{2\mu}{r_p}} \quad (26)$$

where μ is the planet's gravitational constant and r_p is the periapsis radius.

The propellant mass needed to brake the orbiter into a capture orbit ($e < 1$) is given by the rocket equation:

$$\Delta m = m_o(e^{\Delta V/I_{sp}g} - 1) \quad (27)$$

where g is the acceleration due to gravity at the Earth's surface and Δm is the propellant mass.

Table 1 gives the values of ΔV and Δm for Hohmann transfers to each planet, assuming an I_{sp} of 300 s and a 1000 kg orbiter.

4.1. Calculating scale heights

Since the atmospheric drag model used in the tethered aerobraking simulations is exponential in nature, we are assuming that the atmospheric density

Table 1. Hohmann transfers

Body	μ (km^3/s^2)	R (km)	V_∞ (km/s)	r_p (km)†	ΔV (km/s)	Δm (kg)
Venus	3.25×10^5	6.05×10^3	2.71	6190	0.35	126
Earth	3.99×10^5	6.38×10^3	2.97	6480	0.39	142
Mars	4.28×10^4	3.40×10^3	2.65	3490	0.67	256
Jupiter	1.27×10^8	7.14×10^4	5.64	71,900	0.27	96
Saturn	3.79×10^7	6.00×10^4	5.44	60,800	0.41	149
Uranus	5.80×10^6	2.54×10^4	4.66	26,900	0.50	185
Neptune	6.85×10^6	2.43×10^4	4.05	25,500	0.34	122
Titan	9.0×10^3	2.58×10^3	4.01	3080	1.31	559

†Denotes numbers taken from the numerical simulations.

Table 2. Atmospheric parameters

Planet/moon	Composition	Lapse rate dT/dr (K/km)	Ref. r (km)	Ref. ρ (kg/m^3)	Ref. T (K)	g (m/s^2)	Source
Venus	96.5% CO_2 3.5% N_2	N/A†	6150–6180	1.0×10^{-4}– 1.0×10^{-6}	N/A	N/A	[7]
Earth	79% N_2 20% O_2 1% Ar	−4–0	54–91	N/A	165–223	9.81	[6]
Mars	95.7% CO_2 2.7% N_2 1.6% Ar	N/A	90–110	6.03×10^{-7}– 1.6×10^{-7}	N/A	N/A	[8]
Jupiter	89% H_2 11% He	−2–0	71,542– 71,592	N/A	100–133	23.12	[9], [10]
Saturn	94% H_2 6% He	0–0.8	60,308– 60,408	N/A	90–100	8.96	[10], [11], [13]
Uranus	85% H_2 15% He	N/A	26,145	4.7×10^{-2}	59	N/A	[12], [13]
Neptune	85% H_2 15% He	N/A	24,750	5.8×10^{-1}	48	N/A	[12], [13]
Titan	90% N_2 10% CH_4	0.09	2725–2825	N/A	190–200	1.36	[13]

†Information not used (not applicable) in calculating scale heights.

can be written as an exponential function, of the form

$$\rho/\rho_o = e^{-(r-r_o)/H} \tag{28}$$

where H is the scale height. If the value of the scale height is known, and if the atmosphere can be assumed to be locally exponential, then the density can be found at any altitude if given a reference density and altitude, ρ_o and r_o.

Two methods were used to calculate values for H over a range of altitudes at each planet. The first and most direct method requires a density versus altitude plot (or list of data points), and from it the values for H can be found directly by solving eqn (28).

When such information is not available, however, it is necessary to turn to the formal definition of H in order to calculate it, and a full derivation can be found in [6]. Three simple assumptions are made: (1) the atmosphere has exponential behavior, (2) the gases can be approximated as ideal and (3) the rate of change of pressure equals the weight of the atmosphere as the altitude varies. By combining the following two equations,

$$p = \rho RT/m \tag{29}$$

$$dp = -\rho g\, dr \tag{30}$$

and rearranging, we arrive at the following expression:

$$\frac{d\rho}{\rho} = -\left[\frac{gm}{RT} + \frac{1}{T}\frac{dT}{dr}\right] dr \tag{31}$$

If the bracketed term in eqn (31) is defined as $1/H$, then integration will yield eqn (28). In this expression, m is the molecular mass of the atmospheric gases, and g is the local acceleration due to gravity. The term dT/dr is often referred to as the temperature lapse rate, and it gives the change in atmospheric temperature with respect to altitude. This allows H to be calculated when density information is unavailable, as long as pressure and temperature profiles are known.

4.2. *Selected atmospheric properties*

It is necessary to find the scale heights at each planet for altitudes corresponding to the fly-through maneuver. A great deal of information is available for Venus, Mars and Earth; so the application of the atmospheric model is relatively straightforward. However, the information on the outer planets and Titan is sparse, and in some cases existing data had to be extrapolated.

At Venus and Mars, the scale heights are calculated from density profiles, using eqn (28). Earth information is taken directly from Vinh [6]. At Jupiter, Saturn and Titan temperature profiles and lapse data are the primary source of information, and the scale heights are calculated using eqn (31).

Hunt [12] provides scale height information at Uranus without reference to altitude, so it is necessary to use pressure and temperature data in order to locate the reference density and altitude. Due to the similarities between the planets Uranus and Neptune, Neptune's atmosphere is assumed to have properties similar to Uranus since very little Neptune data is available. Table 2 summarizes the atmospheric parameters of the planets and Titan.

The values in Table 3 are considered to be representative of the atmospheric properties of the planets and are used in the numerical simulations. Although there are uncertainties in the scale height and density information, it should be stressed that the design methodology presented in this paper applies to any atmosphere sufficiently dense.

Table 3. Selected atmospheric properties

Body	H (km)	r_o (km)	ρ_o (kg/m^3)
Venus	6	6150	1.0×10^{-4}
Earth	5	6458	7.7×10^{-6}
Mars	8	3507	5.5×10^{-8}
Jupiter	20	71,592	1.85×10^{-3}
Saturn	30	60,350	2.8×10^{-2}
Uranus	40	26,145	4.69×10^{-1}
Neptune	40	24,750	5.76×10^{-1}
Titan	45	2738	1.7×10^{-3}

5. NUMERICAL RESULTS

5.1. Aerocapture at Mars

In this section, a preliminary design of an aerobraking tether for Mars is discussed. A mass of 1000 kg is used for both the orbiter and the probe. The atmosphere of Mars is assumed exponential and its properties are given in Table 3. The aerobraking maneuver involves the deceleration of the tether system from an arrival hyperbolic orbit, determined by the Hohmann trajectory from Earth, to a near parabolic orbit ($e < 1$) around the planet. This maneuver must reduce the velocity by approx. 0.67 km/s (Table 1). Given these preliminary assumptions and the models derived in previous sections, a tether design can be obtained. First, using eqn (12), the mass of the required tether can be calculated given values for the orbiter and probe masses, the ΔV and the tether material properties, where we have chosen $\sigma_u = 3.6\ \mathrm{GN/m^2}$ and $\rho_t = 1800\ \mathrm{kg/m^3}$. In this case a mass of 112 kg is obtained. This compares very favorably with the propellant mass required to capture the orbiter, 256 kg (Table 1). Note that the mass equation requires the matching of the spin rate before and after impact, and that the maneuver must be designed accordingly. Next, center matching and aeromatching requirements are introduced in order to eliminate the normal forces on the tether. The aeromatching requirement [eqn (25)] gives the probe area as a function of the tether length and diameter, which are the only variables remaining in the design (recall that we have assumed that $C_{Dt} = 2$ and $C_{Dp} = 1$). Note that the orbiter area is not an important factor in the design, since the orbiter travels at a higher altitude than the probe and is subjected to much smaller aerodynamic effects. The value used here is $5\ \mathrm{m^2}$. The tether diameter and length can be related using tether mass and density, and the center matching requirement provides the last condition to arrive at a unique design. If the center of pressure and center of percussion are plotted versus tether length

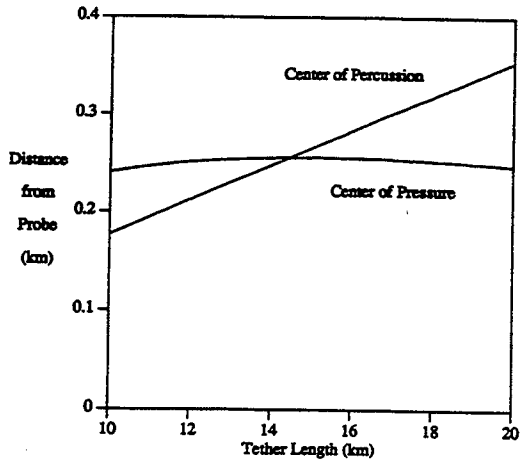

Fig. 5. Tether length based on aeromatching and center matching curves.

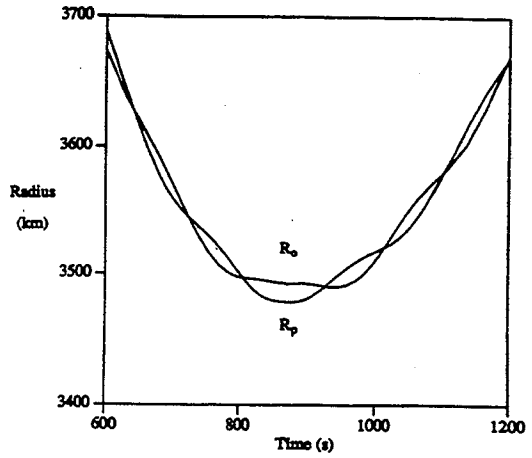

Fig. 6. Orbiter and probe trajectories.

using eqns (14) and (24), the intersection of the two lines represents the tether length that satisfies the aeromatching and center matching requirements (Fig. 5). For the Mars case a length of 14.5 km is obtained. It was found that the tether length is insensitive to variations in ΔV. After the length is found, the tether diameter and probe area are easily computed using eqns (11) and (25). The values obtained are 2.34 mm and $605\ \mathrm{m^2}$, respectively. Note that a unique tether design exists which satisfies all the requirements mentioned above.

The equations derived in [3] are used to simulate the aerobraking maneuver using the tether design described above. The analysis in [3] and [5] provides a method to determine the initial conditions outside the atmosphere required to obtain the desired conditions during atmospheric fly-through. The initial conditions found for the Mars maneuver are:

$$R = 5104.91\ \mathrm{km}$$
$$\alpha = 31.83\ \mathrm{radians}$$
$$\dot{\alpha} = -3.7115 \times 10^{-2}\ \mathrm{r/s}$$

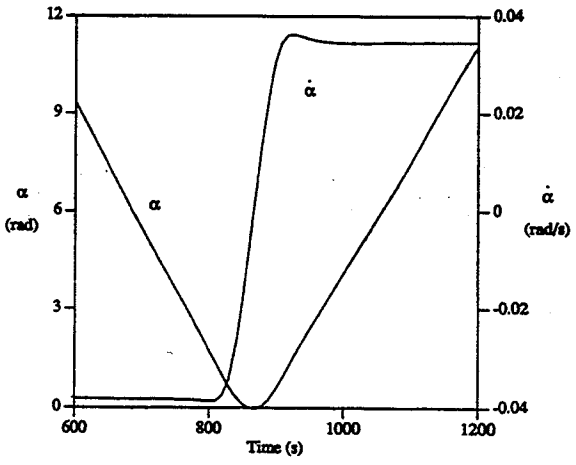

Fig. 7. Orientation angle, α, and $\dot{\alpha}$.

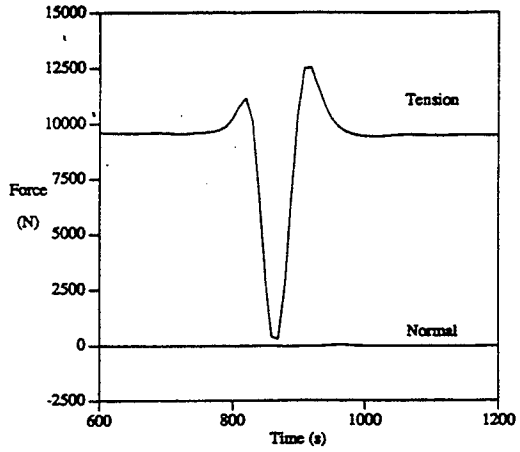

Fig. 8. Tension and normal forces on the orbiter.

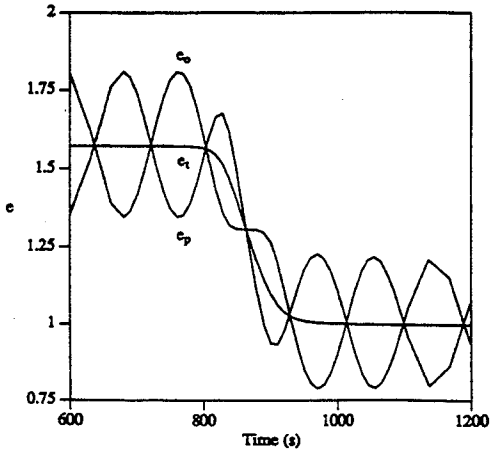

Fig. 10. Eccentricities of tether, orbiter and probe.

where R is the radius from the center of the planet to the center of mass of the tether system and α is the tether orientation angle with respect to the local vertical. The characteristics of the maneuver given by these initial conditions are shown in Figs 6–10. Figure 6 shows the radius of the orbiter and the probe with respect to the center of the planet. Note that the radius of Mars is 3398 km. During atmospheric fly-through the minimum altitudes of the orbiter and the probe are 92.5 and 80.7 km, respectively. The difference between these values is nearly the length of the tether. Next, the orientation of the tether, α, and its spin rate, $\dot{\alpha}$, are shown in Fig. 7. The graph clearly shows that during fly-through the tether remains at a near vertical orientation ($\alpha = 0$). The values of the normal and tension forces at both ends of the tether are plotted in Figs 8 and 9. The graphs clearly show that forces due to spin are equal before and after impact. Also, the normal forces are close to zero, which was one of the goals of the design. Note that the tether designed for this maneuver has an ultimate strength of 15,500 N which is higher than the maximum value of tension observed in the simulation. [The actual tension due to spin is, in this case, overestimated by eqn (10).] Figure 10 shows the eccentricities of the center of mass, and individually of the orbiter and the probe. When the eccentricity of the center of mass is less than unity, then the tether system is guaranteed to be captured. The eccentricities of the orbiter and probe are plotted individually to show when both vehicles would be captured if the tether were severed.

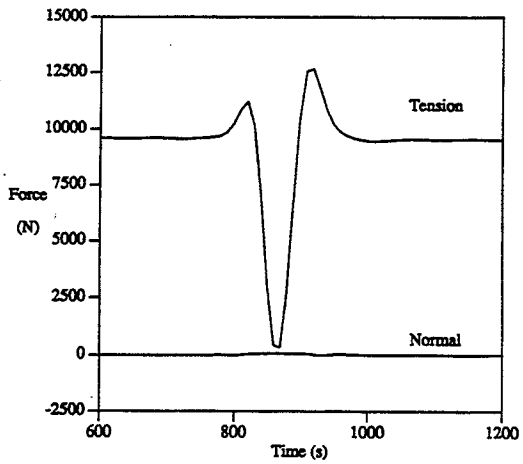

Fig. 9. Tension and normal forces on the probe.

5.2. *Aerocapture results for solar system exploration*

The same process is used to design tethered systems for aerobraking at the other atmosphere-bearing planets and satellites in the solar system. The results of the designs and simulations are summarized in Table 4. The tether masses obtained compare very favorably to the propellant masses in all cases. This fact can be predicted by using eqns (27) and (12), which provide propellant mass and an approximation to tether mass, respectively, as functions of ΔV. In Fig. 11 the two expressions are used to plot mass versus ΔV. Note that the tether mass remains smaller than the propellant mass for all ΔVs below 1.8 km/s. The largest percentage savings are found at Jupiter, but Mars provides the largest absolute savings. The tether length in each case is found to be only a function of the scale height and it is approx. 1.8 H for all the planets. The diameters of the tethers range from 0.5 to 2.3 mm which are reasonable values. The probe areas, on the other hand, are very large, ranging from 605 to 2670 m^2. These values result from the aeromatching requirement and could be reduced with a denser tether material. The tether forces calculated in the design process are very close to those found in the simulation for all cases except for Mars, where the actual forces are significantly smaller, and Neptune, where the actual forces are somewhat larger. The normal forces at both the probe and the orbiter were very small, in accordance with the design specifications for each planet. The difference in minimum altitude between the orbiter and the probe for all cases is nearly the length of the tether. Recalling that the tether length is approx.

Table 4. Aerocapture results for solar system exploration

Values	Venus	Earth	Mars	Jupiter	Saturn	Uranus	Neptune	Titan
ΔV (km/s)	0.35	0.39	0.67	0.27	0.41	0.50	0.34	1.31
Propellant mass (kg)	126	142	256	96	149	185	122	559
Tether mass (kg)	31	38	112	18	42	63	29	426
Savings (%)	75%	73%	56%	81%	72%	66%	76%	24%
Savings (kg)	95	104	144	78	107	122	93	133
Length (km)	10.8	9.0	14.5	36.1	54.4	72.7	72.7	84.2
Diameter (mm)	1.42	1.73	2.34	0.60	0.74	0.78	0.53	1.89
Probe area (m^2)	999	818	605	2370	1910	1810	2670	747
Design tension (N)	5670	8450	15,500	1010	1550	1720	795	10,100
Actual tension (N)	5430	7850	12,700	1050	1630	1860	899	9443
% of design	96%	93%	82%	104%	105%	108%	113%	93%
Orbiter ρ_{max} (kg/m^3)	5.02×10^{-8}	5.39×10^{-8}	2.18×10^{-7}	4.81×10^{-10}	1.73×10^{-9}	3.29×10^{-9}	1.31×10^{-9}	5.21×10^{-7}
Probe ρ_{max} (kg/m^3)	3.04×10^{-7}	3.27×10^{-7}	1.42×10^{-6}	2.92×10^{-9}	1.05×10^{-8}	2.04×10^{-8}	8.14×10^{-9}	2.28×10^{-6}
Orbiter h_{min} (km)	146	103	93	495	848	1496	1246	522
Probe h_{min} (km)	135	94	81	459	794	1423	1173	456

$1.8H$ it is clear why the maximum atmospheric density at the probe is approx. 6 times ($e^{1.8}$ times) larger than that at the orbiter in all cases.

Note that Table 4 presents unique designs based on the requirements given by the rules of thumb developed earlier. Many other designs are possible by eliminating any one of the unique tether design specifications. For example, if greater altitude separation between orbiter and probe is required, this can be achieved by increasing the tether length, but normal forces (and bending) are likely to appear, since center matching is no longer maintained. It is interesting to note that in such a case the tether mass remains the same since it is only dependent on ΔV, as discussed above. The designs in Table 4 provide a useful guideline for all other aerobraking designs, and a way to compare the performance of tether aerocapture systems at the various planets.

6. FUTURE WORK

The ideas presented in this paper suggest several areas for further study. We merely list a few key ones here with some comments.

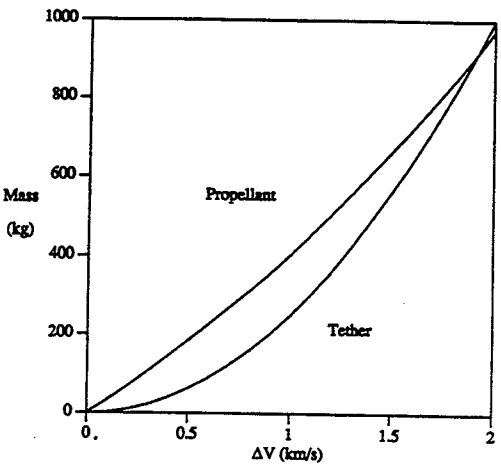

Fig. 11. Tether mass versus propellant mass.

(1) Flexible tether model

In the above analysis, the tether is modeled as a rigid rod, but designed to minimize normal forces. The next logical step is to introduce a flexible tether model to test the virtue of the aforementioned designs. Preliminary results[14] indicate that the flexible behavior is not deleterious to the rigid rod analysis and that the conclusions of the above designs are not appreciably altered. Future analysis with the flexible model will allow a study of how variations in the design will affect normal forces, bending and aerodynamic forces.

(2) Tether guidance and control

An analysis of sensitivity to errors in initial conditions and uncertainties in the atmospheric model will be used to assess the guidance and control issues. Control and guidance of the tether system may include varying the length of the tether in order to control tether orientation and altitude during the atmospheric fly-through. The tether may be severed at a critical time in order to deliver the probe into the atmosphere and the orbiter into a desired orbit. The required accuracy in the timing of the probe release must be analyzed in order to determine what sensors may be necessary to make the system feasible.

(3) Generation of spin rate

In order for the aerobraking tether discussed above to work, a significant spin rate must be imparted to the system. This spin rate represents a large amount of kinetic energy which must be generated somehow. One possibility is to use solar radiation torque to spin up the tether over a long period of time, perhaps during the interplanetary trajectory to the planet. This might be accomplished by an appropriate design of the orbiter and probe exteriors. Another possibility is to use a much longer tether (than the above design) of length l^* with a much smaller initial spin rate. By reeling in the tether, conservation of angular momentum provides the desired high spin rate. In this case,

if the tether were tapered to keep the mass to a minimum, then the extra mass required, Δm_t, is

$$\Delta m_t = \tfrac{1}{2} m_t [1 - (l/l^*)^2] \tag{32}$$

We note that in the limit, as $l^* \to \infty$, the tether mass increases by only 50% over the original design mass.

(4) Mars return mission

A detailed design of a mission to Mars and back to Earth would further illuminate the advantages and disadvantages of the tether aerobraking system. The scale heights of the two planets are not too dissimilar and perhaps the tether could be reeled in for aerocapture on the return to Earth. In such a mission, the tether mass requirements would be greatest at Mars. Other mechanical advantages of the tether would be considered, such as the possibility of using the tether as a sling to propel the vehicle into the outbound and inbound interplanetary trajectories. Naturally this would involve some throw-away mass, such as a spent booster stage. Another consideration in favor of the tether system is that, for a piloted mission, the very long spinning tether would provide a relatively uniform artificial gravity field.

(5) Gravity assist with tethers

A tether could be used on a Voyager-type Grand Tour to deliver spacecraft into orbit about several planets. The lower end of the tether would have a velocity reduction of ΔV while the upper end would have a velocity increase of ΔV. Thus if the ΔV is large enough, the lower vehicle could be dropped into a capture orbit without the need of an atmosphere, while the upper vehicle would continue on a hyperbolic trajectory, with an added boost of ΔV, to the next planet. If the atmosphere of the flyby body is used to either aerobrake the probe or to change the spin rate of the tether, then the system would be referred to as an aerogravity-assist tether. Further analysis will determine if such tethers may increase the number of grand tour opportunities.

7. CONCLUSIONS

The numerical results in this paper indicate that aerobraking tethers may provide significant mass reductions over rocket propulsion systems when used in the exploration of the solar system. Future analysis must consider tether flexibility, spin generation and guidance and control issues.

REFERENCES

1. J. A. Carroll, Tether applications in space transportation. *Acta Astronautica* **13**, 165–174 (1986).
2. E. C. Lorenzini, M. D. Grossi and M. Cosmo, Low altitude tethered Mars probe. *Acta Astronautica* **21**, 1–12 (1990).
3. J. Puig-Suari and J. M. Longuski, Modeling and analysis of tethers in an atmosphere. *Acta Astronautica* **25**, 679–686 (1991).
4. J. M. Longuski and J. Puig-Suari, Hyperbolic aerocapture and elliptic orbit transfer with tethers. IAF Paper No. 91-339 (1991).
5. J. Puig-Suari and J. M. Longuski, Analysis of aerocapture with tethers. AAS Paper No. 91-549 (1991).
6. N. X. Vinh, A. Busemann and R. D. Culp, *Hypersonic and Planetary Entry Flight Mechanics*. The University of Michigan Press, Ann Arbor, MI (1980).
7. A. Seiff, Atmospheres of Earth, Mars, and Venus, as defined by entry probe experiments. *J. Spacecraft Rockets* **28**, 265–275 (1991).
8. A. Kliore (Ed.), The Mars reference atmosphere. COSPAR Working Group 7, Jet Propulsion Laboratory, Pasadena, CA (1978).
9. G. F. Lindal, G. E. Wood, G. S. Levy, J. D. Anderson, D. N. Sweetnam, H. B. Hotz, B. J. Buckles, D. P. Holmes, P. E. Doms, V. R. Eshleman, G. L. Tyler and T. A. Croft, The atmosphere of Jupiter: an analysis of the Voyager radio occultation measurements. *J. Geophys. Res.* **86**, 8721–8727 (1981).
10. G. F. Lindal, D. N. Sweetnam and V. R. Eshleman, The atmosphere of Saturn: an analysis of the Voyager radio occultation measurements. *Astron. J.* **90**, 1136–1144 (1985).
11. G. L. Tyler, V. R. Eshleman, J. D. Anderson, G. S. Levy, G. F. Lindal, G. E. Wood and T. A. Croft, Radio science with Voyager 2 at Saturn: atmosphere and ionosphere and the masses of Mimas, Tethys, and Iapetus. *Science* **215**, 553–557 (1982).
12. G. Hunt (Ed.), *Uranus and the Outer Planets*. Cambridge University Press, Cambridge (1982).
13. W. K. Hartmann, *Moons and Planets*, 2nd edn. Wadsworth, Belmont, CA (1983).
14. J. Puig-Suari and J. M. Longuski, Aerocapture with a flexible tether. AIAA Paper No. 92-4662 (1992).